Macromolecules

Article

pubs.acs.org/Macromolecules

H_2O_2 Enables Convenient Removal of RAFT End-Groups from Block Copolymer Nano-Objects Prepared via Polymerization-Induced Self-Assembly in Water

Craig P. Jesson,[†] Charles M. Pearce,[†] Helene Simon,[†] Arthur Werner,[†] Victoria J. Cunningham,[†] Joseph R. Lovett,[†] Mark J. Smallridge,[‡] Nicholas J. Warren,*[,†] and Steven P. Armes*[,†]

[†]Department of Chemistry, University of Sheffield, Brook Hill, Sheffield S3 7HF, U.K.

[‡]GEO Specialty Chemicals, Hythe, Southampton, Hampshire SO45 3ZG, U.K.

Supporting Information

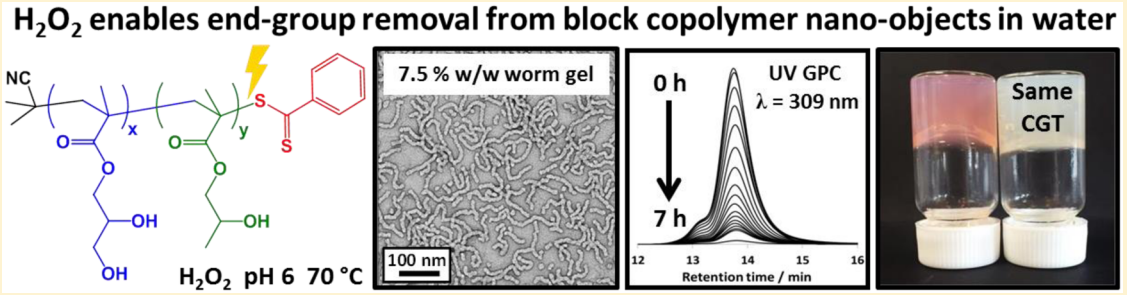

ABSTRACT: RAFT-synthesized polymers are typically colored and malodorous due to the presence of the sulfur-based RAFT end-group(s). In principle, RAFT end-groups can be removed by treating molecularly dissolved copolymer chains with excess free radical initiators, amines, or oxidants. Herein we report a convenient method for the removal of RAFT end-groups from aqueous dispersions of diblock copolymer nano-objects using H_2O_2. This oxidant is relatively cheap, has minimal impact on the copolymer morphology, and produces benign side products that can be readily removed via dialysis. We investigate the efficiency of end-group removal for various diblock copolymer nano-objects prepared with either dithiobenzoate- or trithiocarbonate-based RAFT chain transfer agents. The advantage of using UV GPC rather than UV spectroscopy is demonstrated for assessing both the kinetics and extent of end-group removal.

INTRODUCTION

Over the past two decades reversible addition−fragmentation chain transfer (RAFT) polymerization[1−4] has become a well-established route for the synthesis of a wide range of controlled-structure functional copolymers for various potential applications.[5−10] RAFT polymerization enables good control over target molecular weight, molecular weight distribution, and copolymer architecture, while also providing access to a wide range of specific end-groups.[11−18] The recent development of polymerization-induced self-assembly (PISA) has been based largely on RAFT-mediated polymerization conducted in heterogeneous media.[19−26] PISA has enabled the rational design of a wide range of bespoke block copolymer nanoparticles (e.g., spheres, worms, vesicles, framboidal vesicles, platelets, etc.),[27−30] and certain formulations appear to be promising for potential biomedical applications. For example, poly(glycerol monomethacrylate)−poly(2-hydroxypropyl methacrylate) diblock copolymer worm gels are readily sterilizable via cold ultrafiltration and induce stasis in human embryonic stem cells.[31] Closely related disulfide-functional worm gels are sufficiently robust to enable 3D cell culture for extended periods in plastic matrices.[32] Targeting diblock copolymer vesicles via PISA has enabled encapsulation (and, in some cases, the subsequent release) of various model payloads such as fluorescently labeled water-soluble polymers, silica nanoparticles, or globular proteins, which augurs well for drug delivery applications.[12,33,34]

In the context of potential biomedical and cosmetics applications, one of the main drawbacks of RAFT-synthesized (co)polymers is the color, malodor, and possible toxicity conferred by the sulfur-based end-groups; whether they be dithioesters, trithiocarbonates, or xanthantes,[4] RAFT end-group cleavage via hydrolysis[35,36] (or other chemistries) results in the formation of low molecular weight byproducts that may be preferentially internalized within mammalian cells, apparently without inducing toxicity in at least some cases.[37]

In practice, such problems are often circumvented by pre-emptive removal of the RAFT end-group under controlled conditions. Not surprisingly, this approach works rather better for acrylic (or styrenic) polymers compared to more sterically congested methacrylic polymers.[38,39] Numerous chemistries have been employed, such as aminolysis using either primary

Received: September 7, 2016
Revised: November 17, 2016
Published: December 23, 2016

DOI: 10.1021/acs.macromol.6b01963
Macromolecules 2017, 50, 182−191

amines or hydrazine,[40] ozonolysis,[41] bond cleavage using radicals derived from addition of excess initiator,[42−44] thermolysis,[45,46] or, more recently, light-mediated removal.[47] However, as far as we are aware, there is only one literature report of using H_2O_2 for removing RAFT end-groups, and this brief study was restricted to the derivatization of soluble poly(*N*-vinylpyrrolidone) chains in aqueous solution at 80 °C.[48] A radical mechanism was proposed, whereby hydroxyl radicals generated at elevated temperature replaced each RAFT end-group with a terminal alcohol.

Herein we revisit the use of H_2O_2 as a means of removing RAFT end-groups from various examples of methacrylic diblock copolymer nanoparticles in aqueous solution. In this context, the nonionic nature and relatively low molecular weight of H_2O_2 might be expected to offer a significant advantage in terms of its faster ingress within the nanoparticle interior. Moreover, it is emphasized that H_2O_2 is relatively cheap and produces only water and oxygen as byproducts. It is perhaps also noteworthy that relatively few RAFT end-group derivatization studies have focused on methacrylic copolymers, rather than the more reactive acrylic or styrenic copolymers.

EXPERIMENTAL SECTION

Materials. Glycerol monomethacrylate (GMA, 99.8%), 2-hydroxypropyl methacrylate (HPMA, 99.3%), and benzyl methacrylate (BzMA, 99.2%) were donated by GEO Specialty Chemicals (Hythe, UK) and used without further purification. The synthetic route used to obtain HPMA results in the production of two isomeric forms.[49] The isomeric composition was confirmed by ^{1}H NMR spectroscopy. The "HPMA" monomer actually contained 75 mol % HPMA, with the remainder being its closely related isomer, 2-hydroxyisopropyl methacrylate [HIPMA].

4,4′-Azobis(4-cyanopentanoic acid) (ACVA, 99%) and dichloromethane were purchased from Sigma-Aldrich (UK) and were used as received. 2-Cyano-2-propyldithiobenzoate (CPDB) was purchased from Strem Chemicals Ltd. (Cambridge, UK) and was used as received. 4-Cyano-4-(2-phenylethanesulfanylthiocarbonyl)sulfanylpentanoic acid (PETTC) RAFT agent was synthesized as previously reported.[50] For the sake of brevity, the acronyms DB and TTC are used to denote dithiobenzoate and trithiocarbonate end-groups for the various copolymers prepared in this study. Deuterated DMF and methanol were purchased from Goss Scientific Instruments Ltd. (Crewe, UK). All other solvents were purchased from Fisher Scientific (Loughborough, UK) and used as received. Deionized water was used for all experiments.

Protocol for the Synthesis of PGMA Macro-CTAs. Synthesis of a dithiobenzoate-functionalized poly(glycerol monomethacrylate) $PGMA_{52}$ chain transfer agent is representative of all dithiobenzoate-functionalized macro-CTAs and was prepared as follows. GMA monomer (25.0 g, 156.1 mmol) and CPDB RAFT agent (0.864 g, 3.9 mmol; target degree of polymerization, DP = 40) were weighed into a 100 mL round-bottomed flask and purged under N_2 for 30 min. ACVA initiator (218.6 mg, 0.78 mmol; CTA/ACVA molar ratio = 5.0) and anhydrous ethanol (49.6 mL; previously purged with N_2 for 30 min) were then added, and the resulting red solution was degassed for a further 10 min. The flask was subsequently sealed and immersed into an oil bath set at 70 °C. After 100 min, the GMA polymerization was quenched by exposing to air and immersing in liquid nitrogen for 30 s, followed by dilution with methanol (100 mL). A final GMA conversion of 78% was determined by ^{1}H NMR analysis. The methanolic PGMA solution was precipitated into a ten-fold excess of dichloromethane. After filtration, the crude PGMA precipitate was washed with dichloromethane and dissolved in water, and residual dichloromethane was evaporated under reduced pressure. The resulting aqueous solution was freeze-dried overnight to yield a pink powder. ^{1}H NMR analysis indicated a mean degree of polymerization of 52 for this PGMA-DB macro-CTA (M_n = 15 700, M_w/M_n = 1.18; see Table 1 and Figure S1). This suggests a CTA efficiency of around 60%.

Table 1. Summary of Molecular Weight Data Obtained Using DMF GPC (Refractive Index Detector; vs Poly(methyl methacrylate) Calibration Standards) before and after H_2O_2 Treatment for the Series of Diblock Copolymer Nano-Objects Used in This Study

		M_n /g mol^{-1}		M_w/M_n	
copolymer composition	copolymer morphology	before	after	before	after
G_{52}-DB	dissolved chains	15 700	15 500	1.18	1.19
G_{52}-H_{135}-DB	worms	35 600	35 700	1.12	1.16
G_{52}-H_{135}-TTC	worms	37 400	34 900	1.15	1.20
G_{61}-B_{100}-DB	spheres	15 600	16 800	1.26	1.29
G_{104}-H_{300}-DB	spheres	58 600	56 600	1.19	1.24
G_{104}-H_{600}-DB	spheres	79 100	74 300	1.24	1.28
G_{104}-H_{900}-DB	spheres	136 100	129 500	1.46	1.46
G_{52}-H_{400}-DB	vesicles	101 700	106 300	1.32	1.40

Synthesis of a trithiocarbonate-functionalized $PGMA_{52}$ macro-CTA was performed using PETTC RAFT agent (target degree of polymerization, DP = 55) instead of CPDB via the same general protocol as that described above. A final GMA conversion of 70% was determined by ^{1}H NMR analysis. The crude copolymer was purified via precipitation from methanol into excess dichloromethane to yield a yellow powder. ^{1}H NMR analysis indicated a mean degree of polymerization of 52 for this PGMA-TTC macro-CTA (M_n = 13 700, M_w/M_n = 1.26; see Figure S1). This suggests a CTA efficiency of around 74%.

Synthesis of $PGMA_{104}$−$PHPMA_y$ Diblock Copolymer Spheres. These diblock copolymer nanoparticles were prepared via RAFT aqueous dispersion polymerization, as reported by Blanazs et al.[51] As a typical example, $PGMA_{104}$−$PHPMA_{600}$ spheres were synthesized as follows. $PGMA_{104}$−DB macro-CTA (0.332 g, 19.7 μmol), HPMA monomer (1.70 g, 11.8 mmol; target DP = 600) and ACVA initiator (1.84 mg, 6.55 μmol; macro-CTA/ACVA molar ratio = 3.0) were weighed into a 50 mL round-bottomed flask and dissolved in deionized water (18.3 mL). The resulting solution was purged under N_2 for 30 min before being sealed and immersed in an oil bath at 70 °C for 5 h. The HPMA polymerization was quenched by exposure to air. A final HPMA conversion of more than 99% was determined by ^{1}H NMR analysis. These copolymer spheres were characterized by DMF GPC without further purification and used directly for RAFT end-group removal experiments (M_n = 79 100, M_w/M_n = 1.24; see Figure S2).

Synthesis of $PGMA_{52}$−$PHPMA_{135}$ Diblock Copolymer Worms. These diblock copolymer nanoparticles were prepared via RAFT aqueous dispersion polymerization, as reported by Blanazs et al.[51] A typical protocol used for the PISA synthesis of $PGMA_{52}$−$PHPMA_{135}$ worms was as follows. $PGMA_{52}$ macro-CTA (3.60 g, 0.395 mmol) and HPMA monomer (7.70 g, 53.5 mmol; target DP = 135) were weighed into a 25 mL round-bottomed flask and purged with N_2 for 20 min. ACVA was added (28.3 mg, 0.101 mmol, CTA/ACVA molar ratio = 5.0) and purged with N_2 for a further 5 min. Deionized water (46.1 mL, producing a 20.0% w/w aqueous solution) that had been previously purged with N_2 for 30 min was then added, and the solution was degassed for a further 5 min prior to immersion in an oil bath set at 70 °C. This reaction solution was stirred for 3 h before the polymerization was quenched by exposure to air. These copolymer worms were characterized by DMF GPC without further purification and used directly for RAFT end-group removal experiments (M_n = 35 600, M_w/M_n = 1.12; see Figure S3).

Synthesis of $PGMA_{52}$−$PHPMA_{400}$ Diblock Copolymer Vesicles. These diblock copolymer nanoparticles were prepared via RAFT aqueous dispersion polymerization, as reported by Blanazs et al.[51] $PGMA_{52}$−DB macro-CTA (0.133 g, 15.6 μmol), HPMA

DOI: 10.1021/acs.macromol.6b01963
Macromolecules 2017, 50, 182−191

Scheme 1. Reaction Schemes for (a) the Synthesis of a G_x–H_y–DB Diblock Copolymer via RAFT Aqueous Dispersion Polymerization, (b) the Synthesis of a G_x–H_y–TTC Diblock Copolymer via RAFT Aqueous Dispersion Polymerization, and (c) the Synthesis of a G_x–B_y–DB Diblock Copolymer via RAFT Aqueous Emulsion Polymerization

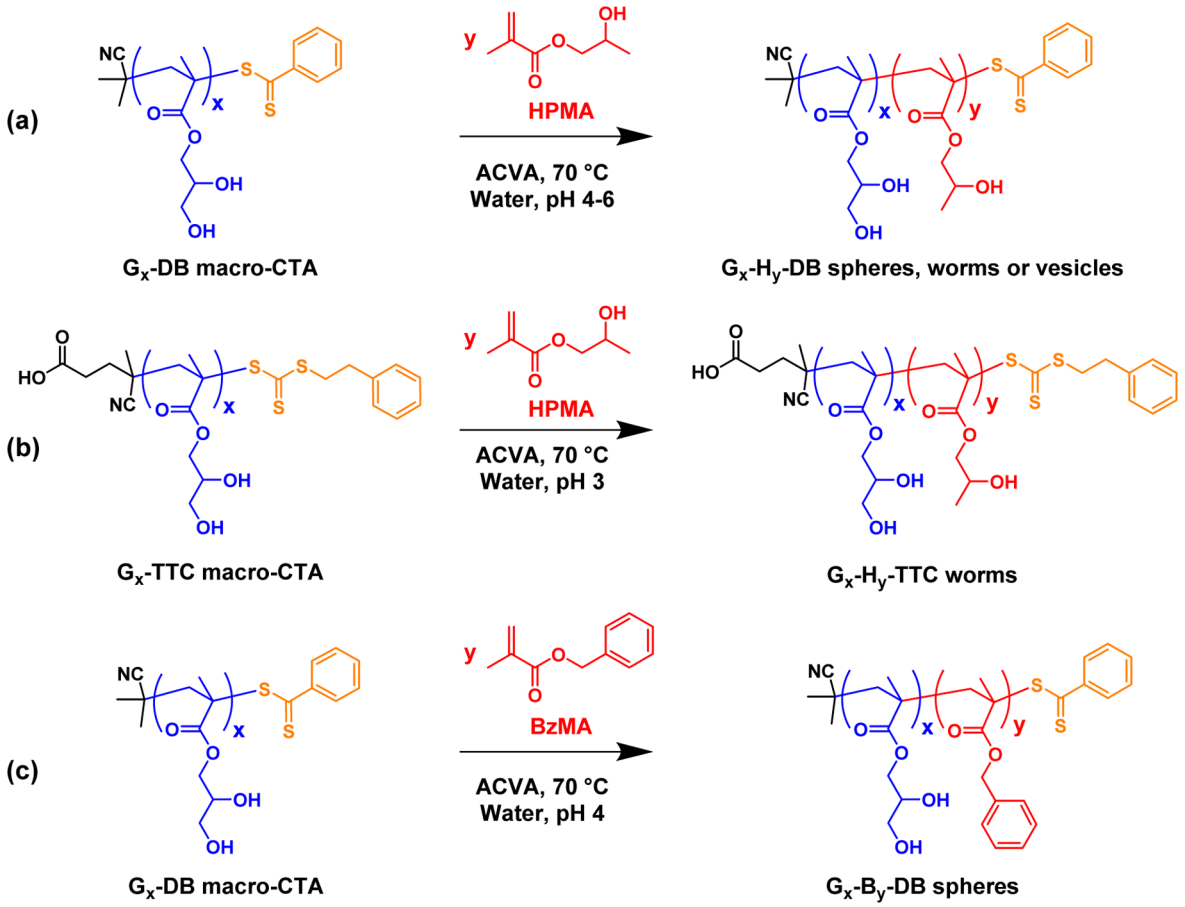

monomer (0.90 g, 6.2 mmol; target DP = 400), and ACVA initiator (1.46 mg, 5.20 μmol, CTA/ACVA molar ratio = 3.0) were weighed into a 25 mL round-bottomed flask and dissolved in deionized water (9.31 mL). The resulting solution was purged under N_2 for 30 min before being sealed and immersed in an oil bath at 70 °C for 4 h. The HPMA polymerization was quenched by exposure to air, and a final HPMA conversion of more than 99% was determined by ^{1}H NMR analysis. These copolymer vesicles were characterized without further purification and used directly for RAFT end-group removal experiments (M_n = 101 700, M_w/M_n = 1.32; see Figure S3).

Synthesis of $PGMA_{61}$–$PBzMA_{100}$ Diblock Copolymer Spheres. These diblock copolymer nanoparticles were prepared via RAFT aqueous emulsion polymerization, as reported by Cunningham et al.[52] $PGMA_{61}$–DB macro-CTA (0.368 g, 36.9 μmol), BzMA monomer (0.65 g, 3.69 mmol; target DP = 100), and ACVA initiator (3.45 mg, 12.3 μmol; macro-CTA/ACVA molar ratio = 3.0) were weighed into a 25 mL round-bottomed flask and dissolved in deionized water (9.19 mL). The resulting solution was purged under N_2 for 30 min before being sealed and immersed in an oil bath at 70 °C for 4 h. The BzMA polymerization was quenched by exposure to air and a final BzMA conversion of more than 99% was determined by ^{1}H NMR analysis. These copolymer spheres were characterized without further purification and used directly for RAFT end-group removal experiments (M_n = 15 600, M_w/M_n = 1.26; see Figure S3).

H_2O_2 Protocol for Cleavage of RAFT End-Groups. The dithiobenzoate end-groups within $PGMA_{104}$–$PHPMA_{600}$ spheres were cleaved as follows: A 10% w/w copolymer dispersion (3.0 mL) was diluted to 7.5% w/w by addition of deionized water (1.0 mL). H_2O_2 (1.48 μL, 14.5 μmol; H_2O_2/CTA molar ratio = 5.0) was added to this dispersion as a 30% w/w aqueous solution. The resulting reaction solution was immersed in an oil bath at 70 °C and left exposed to air. The intrinsic pink coloration disappeared after around 7 h as judged by visual inspection. The trithiocarbonate end-groups on $PGMA_{52}$–$PHPMA_{135}$ worms were cleaved using the same protocol. Visual inspection indicated that the initial yellow coloration almost completely disappeared after 8 h. Preliminary experiments were conducted at pH 6, but subsequent more detailed studies were conducted at pH 3–4, with these lower values arising from the presence of the carboxylic acid-functionalized ACVA initiator and RAFT CTA (PETTC).

NMR Spectroscopy. All ^{1}H NMR spectra were recorded in either deuterated methanol (for the PGMA macro-CTAs and PGMA–PHPMA diblock copolymers) or deuterated DMF (for the PGMA–PBzMA diblock copolymers) using a 400 MHz Bruker Avance-400 spectrometer (64 scans averaged per spectrum).

Gel Permeation Chromatography (GPC). Copolymer molecular weights and polydispersities were determined using an Agilent 1260 Infinity GPC system equipped with both refractive index and UV–vis detectors. Two Agilent PL gel 5 μm Mixed-C columns and a guard column were connected in series and maintained at 60 °C. HPLC-grade DMF containing 10 mM LiBr was used as eluent, and the flow rate was set at 1.0 mL min^{-1}. DMSO was used as a flow-rate marker. The refractive index detector was used for calculation of molecular weights and polydispersities by calibration using a series of ten near-monodisperse poly(methyl methacrylate) standards (with M_n values ranging from 625 to 618 000 g mol^{-1}). UV GPC chromatograms were obtained simultaneously by detection at a fixed wavelength of 309 nm which corresponds to the absorption maximum assigned to the dithiobenzoate or trithiocarbonate RAFT end-groups.

UV–Vis Absorption Spectroscopy. Absorption spectra were recorded between 200 and 800 nm using a Shimadzu UV-1800

DOI: 10.1021/acs.macromol.6b01963
Macromolecules 2017, 50, 182–191

spectrophotometer. For kinetic studies, 0.10 mL aliquots were diluted ten-fold by addition of methanol (0.90 mL). Measurements were also conducted on purified freeze-dried copolymers after redispersing in water at either 0.25 or 5.00 mg mL^{-1} in order to observe absorption maxima at 309 and 550 nm, respectively.

Transmission Electron Microscopy (TEM). Copolymer dispersions were diluted fifty-fold at 20 °C to generate 0.20% w/w dispersions. Copper/palladium TEM grids (Agar Scientific, UK) were coated in-house to produce a thin film of amorphous carbon. These grids were then treated with a plasma glow discharge for 30 s to create a hydrophilic surface. Each aqueous diblock copolymer dispersion (12 μL; 0.20% w/w) was placed on a freshly treated grid for 1 min and then blotted with filter paper to remove excess solution. To stain the deposited nanoparticles, an aqueous solution of uranyl formate (9 μL; 0.75% w/w) was placed on the sample-loaded grid via a micropipet for 20 s and then carefully blotted to remove excess stain. Each grid was then carefully dried using a vacuum hose. Imaging was performed using a FEI Tecnai Spirit TEM instrument equipped with a Gatan 1kMS600CW CCD camera operating at 120 kV.

Oscillatory Rheology Experiments. An AR-G2 rheometer equipped with a variable temperature Peltier plate, a 40 mL 2° aluminum cone, and a solvent trap was used for all experiments. Temperature sweeps were conducted at an angular frequency of 1.0 rad s^{-1} and a constant strain of 1.0%. The temperature was increased by 1.0 °C between each measurement, allowing an equilibration time of 2 min in each case. A solvent trap was required to prevent evaporation of water over the time scale of these experiments.

RESULTS AND DISCUSSION

A series of PISA-synthesized diblock copolymer nano-objects were examined in this study. These nano-objects were carefully selected in order to enable various comparisons to be made. In particular, we wished to explore (i) the effect of varying the particle diameter for a series of spherical nanoparticles, (ii) the effect of copolymer morphology (i.e., spheres vs worms vs vesicles), (iii) the extent to which a more hydrophobic core-forming block retarded ingress of the H_2O_2 reagent, and (iv) whether trithiocarbonate end-groups could be removed as readily as dithiobenzoate end-groups from otherwise identical nano-objects. For the sake of brevity, the three PGMA, PHPMA, and PBzMA blocks investigated in this study are abbreviated to G, H, and B in all of the figures and tables, with the mean degrees of polymerization of each block being indicated in subscript.

Recently, we have designed a range of thermoresponsive PGMA–PHPMA worm gels for various biomedical applications, including highly biocompatible 3D cell culture matrices,[32,53] induction of stasis in human stem cell colonies,[31] and the cryopreservation of red blood cells.[54] For such biomaterials, the removal of RAFT end-groups is likely to be important for FDA approval, so in our initial experiments we focused on one such system.

For the preparation of the PGMA–PHPMA–DB worm gel examined in this study, HPMA was polymerized using a well-defined $PGMA_{52}$–DB macro-CTA to almost full conversion (>99%, see Scheme 1a), as indicated by the disappearance of the vinyl proton signals at 5.5 and 6.2 ppm. According to ^1H NMR spectroscopy, the mean diblock copolymer composition was calculated to be $PGMA_{52}$–$PHPMA_{135}$. DMF GPC analysis (refractive index detector against poly(methyl methacrylate)) standards indicated that this diblock copolymer had an M_n of 35 600 g mol^{-1} and an M_w/M_n of 1.12.

Initial attempts to cleave RAFT end-groups involved treating a 7.5% w/w $PGMA_{52}$–$PHPMA_{135}$–DB worm gel with various amounts of H_2O_2 in the presence of air at 70 °C (see Scheme 2). In each case, UV–vis absorption spectra were recorded after diluting the aqueous dispersion ten-fold with methanol to produce 9:1 methanol/water solutions. Normalized absorbance vs time plots (see Figure 1) indicated that more than 90% of dithiobenzoate end-groups could be removed using a H_2O_2/dithiobenzoate molar ratio of either 5.0 or 10.0. Lower molar ratios required rather long reaction times, whereas higher molar ratios led to the evolution of a high molecular weight shoulder in the GPC chromatogram (see Figure S4) and also produced subtle differences in the copolymer worm rheology (see Figure S5). On the basis of these preliminary experiments, a H_2O_2/dithiobenzoate molar ratio of 5.0 was selected for more detailed studies.

Scheme 2. Proposed Reaction Scheme for the Removal of Dithiobenzoate End-Groups from $PGMA_x$–$PHPMA_y$ Diblock Copolymer Nano-Objects Using H_2O_2 in Water

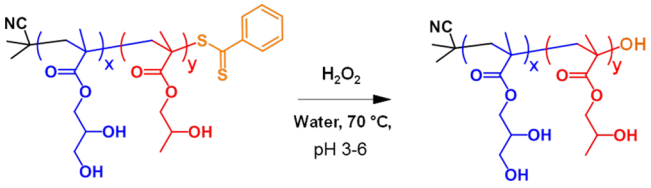

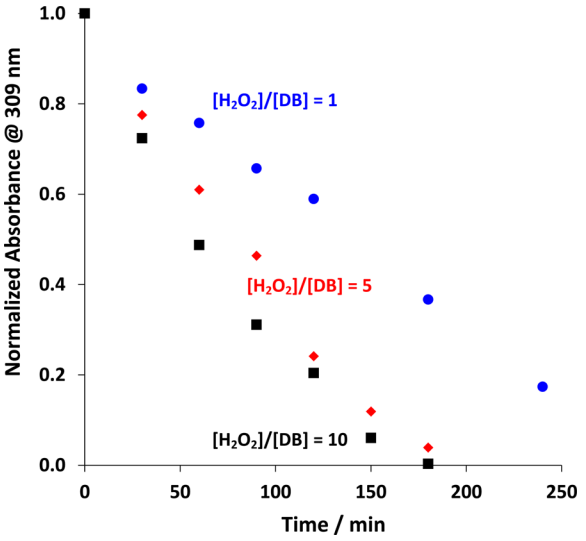

Figure 1. Normalized absorbance plots obtained using UV spectroscopy for the rate of removal of dithiobenzoate (DB) end-groups from 7.5% w/w aqueous dispersions of poly(glycerol monomethacrylate)–poly(2-hydroxypropyl methacrylate) (G_{52}–H_{135}–DB) worms. These data sets were obtained by monitoring the progressive attenuation of the UV absorption (λ_{max} = 309 nm) using the stated H_2O_2/DB molar ratios at 70 °C and pH 4–6.

End-group removal for a 7.5% w/w aqueous dispersion of $PGMA_{52}$–$PHPMA_{135}$–DB worms using a H_2O_2/dithiobenzoate molar ratio of 5.0 was repeated on a gram scale to enable full characterization. Visual inspection indicated almost complete removal of the initial pink coloration, producing a white dispersion after 2 h at 70 °C. After purification by dialysis, ^1H NMR studies indicated disappearance of the aromatic signals at 7.5–8.0 ppm assigned to the dithiobenzoate group (see Figure 1a), suggesting successful end-group removal. Comparison of the remaining integrated copolymer signals suggests little effect on the overall copolymer composition. DMF GPC chromatograms obtained for

DOI: 10.1021/acs.macromol.6b01963
Macromolecules 2017, 50, 182–191

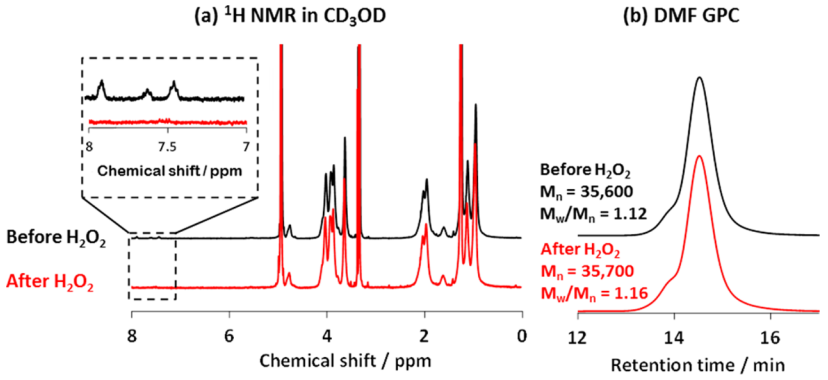

Figure 2. (a) ^{1}H NMR spectra recorded before and after removal of the dithiobenzoate (DB) end-group from a 7.5% w/w G_{52}–H_{135} diblock copolymer aqueous dispersion by exposure to H_2O_2 for 160 min in water (pH 4–6, 70 °C) using a $[H_2O_2]/[DB]$ molar ratio of 5.0; (b) Molecular weight distributions obtained via DMF GPC (refractive index detector, calibrated against poly(methyl methacrylate) standards) for a G_{52}-H_{135} diblock copolymer before and after treatment with H_2O_2 under the conditions stated in (a).

$PGMA_{52}$–$PHPMA_{135}$ before and after H_2O_2 treatment are similar, although a weak high molecular weight shoulder becomes slightly more prominent (see Figure 2b). However, there is only a minimal change in M_n (from 35 600 to 35 700 g mol^{-1}) and M_w/M_n (from 1.12 to 1.16), suggesting that the original copolymer molecular weight distribution is essentially unaffected.

The white powder produced on freeze-drying the purified copolymer was dissolved in methanol and analyzed by UV–vis spectroscopy in order to assess the extent of end-group removal (see Figure 3a). Methanol is a good solvent for both the PGMA and PHPMA blocks; this protocol ensures molecular dissolution of the copolymer chains and hence eliminates any light scattering effects on the spectra. Dithiobenzoate end-groups exhibit a characteristic absorbance at 309 nm, which is clearly visible in the original $PGMA_{52}$–$PHPMA_{135}$ copolymer spectrum. H_2O_2 treatment of the aqueous copolymer dispersion (H_2O_2/dithiobenzoate molar ratio = 5.0; 70 °C for 160 min) leads to almost complete disappearance of this 309 nm signal. However, a relatively weak new absorption appears at approximately 270 nm, which prevents the absorbance at 309 nm falling to zero. The origin of this new spectral feature is currently unclear and probably warrants further studies. Similar observations are made in the corresponding visible region of the same spectra (Figure 3b): the much weaker absorption located at around 509 nm almost completely disappears. This is consistent with the digital images shown in Figure 3c, which confirm the complete removal of the pink coloration from the freeze-dried copolymer powder. Moreover, a tube inversion test indicated that thermoreversible degelation can still be induced on cooling a reconstituted H_2O_2-treated copolymer worm gel from 37 to 2 °C. These observations were confirmed using variable temperature oscillatory rheology studies (Figure 4). Moreover, such gel rheology studies are almost identical to the data set obtained for the original worm gel prior to H_2O_2 treatment. In particular, there is almost no change in the gel modulus, G', at 37 °C or in the critical gelation temperature (CGT) for this worm gel.

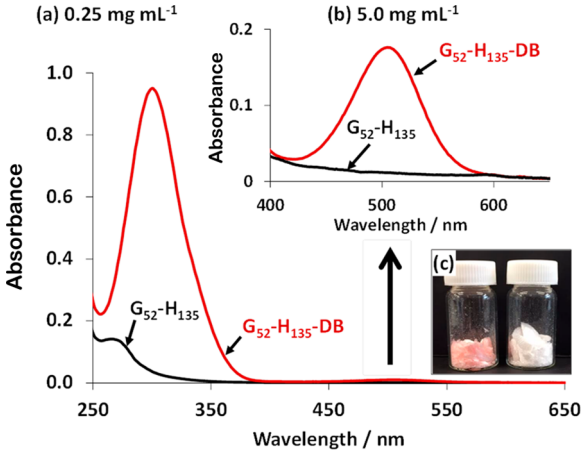

Figure 3. (a) UV–vis absorption spectra recorded for 0.25 mg mL^{-1} G_{52}–H_{135} diblock copolymer solutions in methanol before and after dithiobenzoate end-group removal ($[H_2O_2]/[DB]$ = 5.0, 70 °C, 160 min). (b) Visible absorption spectra obtained for the same copolymers at 5.0 mg mL^{-1} in methanol indicating the disappearance of the relatively weak absorption band at approximately 500 nm (which corresponds to the intrinsic pink color conferred by the RAFT chain-end). (c) Digital image showing the freeze-dried G_{52}–H_{135} copolymer before and after dithiobenzoate end-group removal.

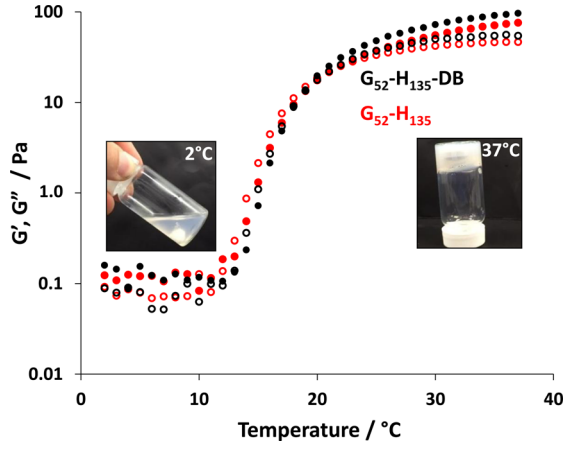

Figure 4. Temperature-dependent oscillatory rheology studies on a 10% w/w G_{52}–H_{135} worm gel before (G_{52}–H_{135}–DB) and after (G_{52}–H_{135}) treatment with H_2O_2 to remove the dithiobenzoate chain-ends. The freeze-dried powder was redispersed in cold 150 mM PBS at 2 °C. Inset digital images show a 10% w/w dispersion of the reconstituted G_{52}–H_{135} copolymer after end-group removal as a free-flowing liquid at 2 °C and a free-standing gel at 37 °C.

DOI: 10.1021/acs.macromol.6b01963
Macromolecules 2017, 50, 182–191

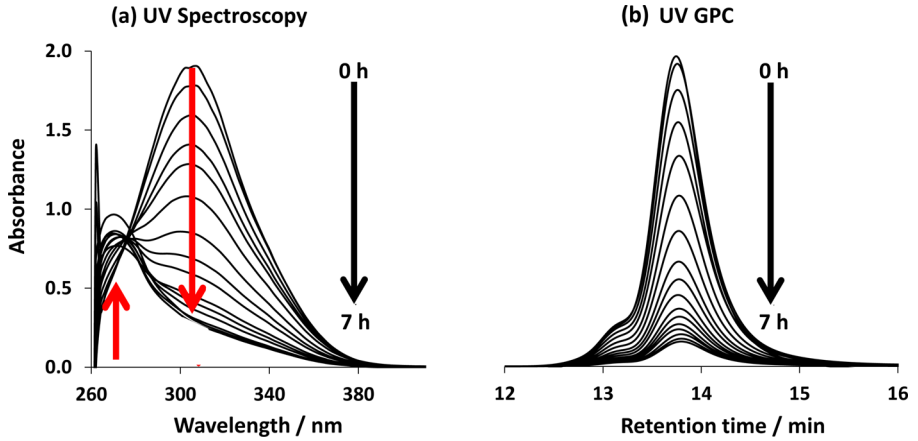

Figure 5. (a) UV spectra and (b) UV GPC chromatograms (recorded at a λ_{max} of 309 nm) obtained during kinetic studies of the removal of dithiobenzoate end-groups from a 7.5% w/w G_{104}–H_{300} aqueous dispersion of spheres using a H_2O_2/dithiobenzoate molar ratio of 5.0 at 70 °C in water (pH 3–4). All GPC samples were diluted to 7.5 mg mL^{-1} prior to analysis.

The kinetics of dithiobenzoate end-group removal at 70 °C from H_2O_2-treated $PGMA_{104}$–$PHPMA_{300}$–DB spheres was conducted by extracting a series of aliquots from the 7.5% w/w copolymer dispersion after various time periods and subsequently diluting ten-fold with methanol (to produce a 9:1 methanol/water solution) prior to analysis by UV–vis spectroscopy at 20 °C. As expected, gradual attenuation in the 309 nm absorption band was initially observed (see Figure 5a). However, apparently no further reduction occurred after approximately 6 h. Inspecting the evolution in UV spectra more closely, this artifact appears to be the result of an additional spectral feature at 270 nm, which is associated with the formation of unknown low molecular weight degradation products (e.g. possibly benzoic acid). In order to circumvent this problem, further end-group removal studies were conducted using UV GPC analysis. By setting the UV detector to a fixed wavelength of 309 nm, it was possible to monitor the extent of end-group removal for copolymer chains bearing either a dithiobenzoate or a trithiocarbonate end-group. The decisive advantage of this approach is that fractionation of the copolymer chains from the small molecule impurities occurs in the GPC column prior to analysis. Thus, there is no longer any interference from the small molecule impurities absorbing at shorter wavelengths, which aids quantification. For this particular data set, an overall 96% reduction in the original UV signal was observed within 8 h (see Figure 5b). At this point, we examined whether full end-group removal could be achieved given a sufficiently long reaction time. Thus, the H_2O_2 treatment was extended from 8 to 24 h at 70 °C, which led to an overall reduction in the original UV GPC signal of 98% (see Figure S6).

Applying this optimized analytical protocol to the $PGMA_{52}$–$PHPMA_{135}$–DB worms (see above) indicated a 95% reduction in RAFT end-group concentration within 2.5 h at 70 °C. Moreover, the rate of end-group removal achieved for this aqueous dispersion of copolymer worms was comparable to that achieved for a water-soluble dithiobenzoate $PGMA_{52}$–DB homopolymer precursor under the same conditions (i.e., same molar concentration of dithiobenzoate groups) (see Figure 6). This indicates that the H_2O_2 reagent can readily access the dithiobenzoate end-groups within the weakly hydrophobic PHPMA cores, which is consistent with the partially hydrated nature of these core-forming chains.[53] Essentially the same

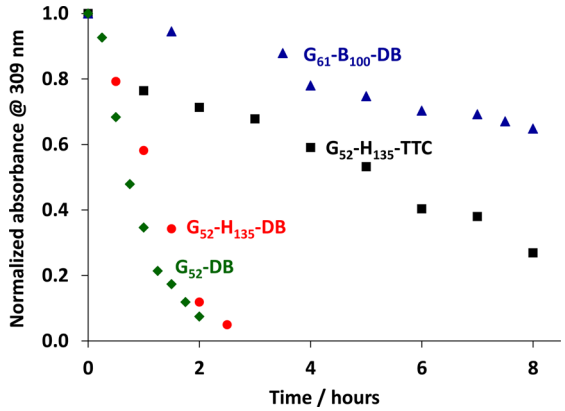

Figure 6. Kinetic plots for the rate of removal of dithiobenzoate or trithiocarbonate end-groups using a [H_2O_2]:[end-group] molar ratio of 5.0 at 70 °C and pH 3–4. (a) 7.5% w/w dithiobenzoate-terminated poly(glycerol monomethacrylate)–poly(benzyl methacrylate) (G_{61}–B_{100}) spheres of 24 nm diameter; (b) 7.5% w/w trithiocarbonate-terminated poly(glycerol monomethacrylate)–poly(2-hydroxypropyl methacrylate) worms (G_{52}–H_{135}–TTC); (c) 7.5% w/w dithiobenzoate-terminated poly(glycerol monomethacrylate)–poly(2-hydroxypropyl methacrylate) worms (G_{52}–H_{135}–DB); (d) 2.3% w/w (equimolar to G_{52}–H_{135}–DB) dithiobenzoate-terminated molecularly dissolved poly(glycerol monomethacrylate) chains (G_{52}–DB).

$PGMA_{52}$–$PHPMA_{135}$–TTC diblock copolymer worms (M_n = 37 400 g mol^{-1}, M_w/M_n = 1.15) were also prepared at 10% w/w solids using PETTC (see Scheme 1b), which is a well-known trithiocarbonate-based RAFT agent.[55] On dilution, the resulting 7.5% w/w copolymer worm dispersion was also treated with H_2O_2 under identical conditions as those utilized for the dithiobenzoate-functionalized copolymer worms. However, the kinetic data obtained by monitoring the UV GPC signal at 309 nm suggest that trithiocarbonate cleavage proceeded significantly more slowly than dithiobenzoate cleavage, with only around 76% end-group removal being achieved within 8 h at 70 °C (see Figure 6). This was not unexpected given that trithiocarbonates are known to exhibit greater hydrolytic stability compared to dithiobenzoates.[35] The effect of varying the nature of the core-forming chains on the extent of end-group removal was also investigated by replacing the PHPMA block with the more hydrophobic PBzMA block. More specifically, a dithiobenzoate-based $PGMA_{61}$–DB macro-CTA

DOI: 10.1021/acs.macromol.6b01963
Macromolecules 2017, 50, 182–191

was used to prepare $PGMA_{61}$–$PBzMA_{100}$–DB spheres via RAFT aqueous emulsion polymerization (see Scheme 1c) according to a protocol recently reported by Cunningham and co-workers.[52] This diblock composition was selected so that the mean diameter of these spheres was approximately 25 nm, which is comparable to the mean width of the dithiobenzoate-based $PGMA_{52}$–$PHPMA_{135}$ worms (as estimated by TEM studies). On treating these $PGMA_{61}$–$PBzMA_{100}$–DB spheres with H_2O_2, the rate of end-group removal was found to be very slow, with 60% of end-groups remaining after 8 h as judged by UV GPC (see Figure 6). This suggests that, despite its nonionic nature and relatively low molecular weight, diffusion of the H_2O_2 reagent into the PBzMA cores is severely retarded compared to PHPMA cores.

In a related series of experiments, three examples of $PGMA_{104}$–$PHPMA_x$–DB spheres (where x = 300, 600, or 900, corresponding to mean DLS hydrodynamic diameters of 54, 81, and 117 nm, respectively) were also subjected to H_2O_2 treatment followed by UV GPC analysis (see Figure 7). The

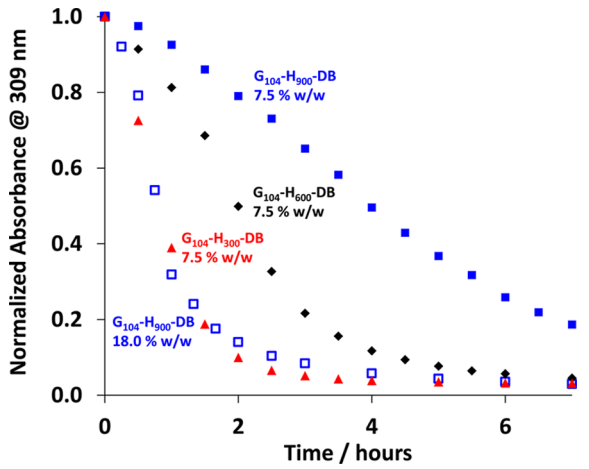

Figure 7. Kinetic plots for the rate of removal of dithiobenzoate end-groups from four poly(glycerol monomethacrylate)–poly(2-hydroxypropyl methacrylate) (G_{104}–H_y) aqueous dispersions as judged by UV GPC analysis (λ_{max} = 309 nm) using a [H_2O_2]:[end-group] molar ratio of 5.0 at 70 °C and pH 3–4. (a) 7.5% w/w G_{104}–H_{300} spheres of 51 nm diameter; (b) 7.5% w/w G_{104}–H_{600} spheres of 81 nm diameter; (c) 7.5% w/w G_{104}–H_{900} spheres of 117 nm diameter; (d) 18.0% w/w G_{104}–H_{900} spheres of 117 nm diameter.

purpose of these experiments was to examine whether particle size had any effect on the rate of end-group removal. Normally, slower H_2O_2 ingress might be expected for larger particles, but if the PHPMA cores are relatively hydrated, then in principle there might be no physical barrier to the diffusion of this reagent.

H_2O_2 treatment (using a H_2O_2/dithiobenzoate molar ratio of 5.0 at 70 °C) of these $PGMA_{104}$–$PHPMA_{300-900}$–DB spheres at a fixed 7.5% w/w copolymer concentration led to a significant reduction in the rate of end-group removal with increasing PHPMA DP (see Figure 7). At first sight, this suggests a slower rate of H_2O_2 ingress into the larger spheres. However, targeting a higher DP at the same fixed copolymer concentration inevitably means a lower concentration of dithiobenzoate end-groups. Comparing the rate of end-group cleavage for $PGMA_{104}$–$PHPMA_{300}$ spheres at 7.5% w/w with that for $PGMA_{104}$–$PHPMA_{900}$ spheres at 18.0% w/w (i.e., at the same *molar* concentration of dithiobenzoate end-groups) indicates essentially no difference in kinetics (see Figure 7). This confirms that the partially hydrated PHPMA cores of this series of spheres offer no diffusional barrier to H_2O_2 ingress, at least for the particle size range investigated herein.

Finally, 10% w/w aqueous dispersions of $PGMA_{104}$–$PHPMA_{600}$–DB spheres, $PGMA_{52}$–$PHPMA_{135}$–DB worms, and $PGMA_{58}$–$PHPMA_{400}$–DB vesicles were each subjected to H_2O_2 treatment (H_2O_2/dithiobenzoate molar ratio = 5.0; 70 °C for 3 h). In each case a high degree of decolorization was observed, indicating almost complete cleavage of the dithiobenzoate end-groups (see digital images shown in Figure 8). Moreover, it is perhaps worth emphasizing that if any loss of RAFT end-groups did occur during such PISA syntheses, then the relatively low levels (2–5% in most cases) of residual RAFT end-groups determined by UV GPC analysis actually represent upper limit values. TEM studies confirmed that this derivatization protocol produced no discernible effect on the copolymer morphology, with comparable images being obtained before and after H_2O_2 treatment in each case (Figure 8). Moreover, DMF GPC analysis (using a refractive index detector) indicated only minimal changes (often within experimental error) in the M_n values obtained for each of the seven H_2O_2-treated diblock copolymers examined in this study and also a $PGMA_{52}$–DB macro-CTA control (see Table 1 and also Figure S7). The M_w/M_n values are typically slightly higher after derivatization, but overall the extent of chemical degradation appears to be negligible. Longer reaction times of up to 7 h also led to no discernible change in the GPC chromatograms recorded for $PGMA_{104}$–$PHPMA_{300-900}$–DB spheres (see Figure S8).

Although a hydroxyl radical mechanism was proposed by Pfukwa and co-workers,[48] the following observations indicate that an *oxidation* mechanism may be more likely, at least under the end-group cleavage conditions described herein. Two identical batches of the same dithiobenzoate-functionalized $PGMA_{52}$–$PHPMA_{135}$ copolymer were subjected to end-group removal using H_2O_2 (H_2O_2/dithiobenzoate molar ratio = 5.0; 7.5% w/w copolymer dispersion; 70 °C). One batch was degassed for 30 min using N_2 prior to end-group removal, with UV–vis spectroscopy studies indicating that dithiobenzoate cleavage was complete within about 240 min. In contrast, the second batch was not degassed and remained exposed to air during the H_2O_2 reaction. In this case, dithiobenzoate cleavage was complete within 150 min (see Figure S9). This rate acceleration in the presence of oxygen is consistent with an oxidative mechanism. Moreover, oxygen is a well-known retarder of radical-based reactions (e.g., free radical polymerizations or RAFT polymerizations). In summary, we suggest that H_2O_2-mediated end-group removal may proceed via an oxidative mechanism rather than a radical mechanism. Further studies are required to establish the precise nature of the end-groups that are formed after H_2O_2 treatment, although Pfukwa and co-workers[48] present some indirect evidence that terminal hydroxyl groups may be formed, at least in the case of poly(*N*-vinylpyrrolidone) prepared using a xanthate-based RAFT agent.

CONCLUSIONS

H_2O_2 can be utilized as a relatively cheap reagent for the convenient and efficient removal of dithiobenzoate end-groups from $PGMA_x$–$PHPMA_y$ diblock copolymer nano-objects in concentrated aqueous solution. The original spherical, worm-like, or vesicular copolymer morphologies are retained after this chemical derivatization, and UV GPC analysis indicates that

DOI: 10.1021/acs.macromol.6b01963
Macromolecules 2017, 50, 182–191

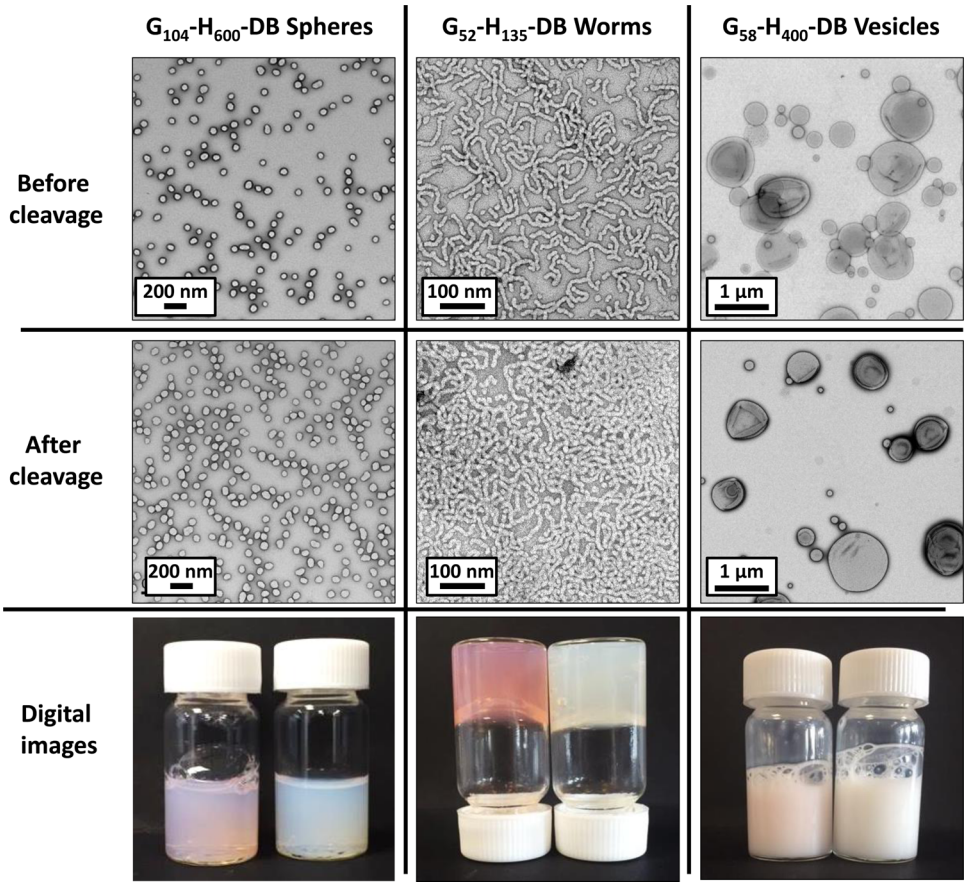

Figure 8. TEM and digital images recorded for 10% w/w aqueous copolymer dispersions of G_{104}−H_{600} spheres, G_{52}−H_{135} worms, and G_{58}−H_{400} vesicles before and after treatment using H_2O_2 at a $[H_2O_2]/[DB]$ molar ratio of 5.0 for 3 h at 70 °C and pH 3−4.

approximately 96% of dithiobenzoate end-groups can be removed within 8 h at 70 °C when using a H_2O_2/dithiobenzoate molar ratio of 5.0. Moreover, H_2O_2 treatment of a series of $PGMA_{104}$−$PHPMA_x$−DB spheres indicates that the rate of end-group removal was both independent of particle size and comparable to that observed for a water-soluble $PGMA_{52}$−DB homopolymer under the same conditions. This suggests that the highly hydrated nature of the weakly hydrophobic PHPMA core-forming chains does not inhibit H_2O_2 diffusion.

Oscillatory rheology studies confirm that removal of dithiobenzoate end-groups does not adversely affect the thermoresponsive gelation behavior exhibited by $PGMA_{52}$−$PHPMA_{135}$ worms in aqueous solution. However, end-group removal is much less effective for dithiobenzoate-functionalized $PGMA_{61}$−$PBzMA_{100}$ spheres, with less than 40% of these RAFT chain-ends being cleaved within 8 h at 70 °C using the same H_2O_2/dithiobenzoate molar ratio. This marked difference simply reflects the retarded diffusion of the H_2O_2 reagent into the relatively dehydrated hydrophobic PBzMA cores. It is also clear from this study that trithiocarbonate end-groups are significantly more resistant to H_2O_2 cleavage than dithiobenzoate end-groups under the same conditions. Finally, it is emphasized that UV GPC analysis in DMF is much more useful than UV−visible spectroscopy analysis of aqueous dispersions for monitoring the rate of RAFT end-group removal. This is because the former technique separates the copolymer chains from small moelcule impurities prior to analysis, which eleminates spectral interference from the latter species.

■ ASSOCIATED CONTENT

Supporting Information

The Supporting Information is available free of charge on the ACS Publications website at DOI: 10.1021/acs.macromol.6b01963.

Figures S1−S9 (PDF)

■ AUTHOR INFORMATION

Corresponding Authors

*E-mail n.warren@leeds.ac.uk (N.J.W.).
*E-mail s.p.armes@shef.ac.uk (S.P.A.).

ORCID

Steven P. Armes: 0000-0002-8289-6351

Present Address

N.J.W.: School of Chemical and Process Engineering, University of Leeds, Woodhouse Lane, Leeds, Yorkshire, LS2 9JT, UK.

Notes

The authors declare no competing financial interest.

■ ACKNOWLEDGMENTS

GEO Specialty Chemicals (Hythe, UK) is thanked for supplying the GMA, HPMA, and BzMA monomers and also for part-funding PhD studentships for J.R.L. and C.P.J. EPSRC is also thanked for funding a CDT studentship for C.P.J. EPSRC is thanked for postdoctoral support of N.J.W. (EP/L024160/1). The Royal Society of Chemistry is thanked for funding a summer studentship for C.M.P. GE Healthcare

DOI: 10.1021/acs.macromol.6b01963
Macromolecules 2017, 50, 182−191

(Cardiff, UK) is thanked for funding a summer internship for A.W. S.P.A. is the recipient of a five-year ERC Advanced Investigator grant (PISA 320372).

REFERENCES

(1) Chiefari, J.; Chong, Y. K.; Ercole, F.; Krstina, J.; Jeffery, J.; Le, T. P. T.; Mayadunne, R. T. A.; Meijs, G. F.; Moad, C. L.; Moad, G.; Rizzardo, E.; Thang, S. H. Living free-radical polymerization by reversible addition-fragmentation chain transfer: The RAFT process. *Macromolecules* **1998**, *31*, 5559.
(2) Moad, G.; Rizzardo, E.; Thang, S. H. Living Radical Polymerization by the RAFT Process. *Aust. J. Chem.* **2005**, *58*, 379.
(3) Moad, G.; Rizzardo, E.; Thang, S. H. Living Radical Polymerization by the RAFT Process - A Second Update. *Aust. J. Chem.* **2009**, *62*, 1402.
(4) Moad, G.; Rizzardo, E.; Thang, S. H. Living Radical Polymerization by the RAFT Process - A Third Update. *Aust. J. Chem.* **2012**, *65*, 985.
(5) Fairbanks, B. D.; Gunatillake, P. A.; Meagher, L. Biomedical applications of polymers derived by reversible addition - fragmentation chain-transfer (RAFT). *Adv. Drug Delivery Rev.* **2015**, *91*, 141.
(6) Price, D.; Mosier, P. E.; Vilardo, J. S.; Baum, M. The Lubrizol Corporation, 2013.
(7) Loiseau, J.; Doerr, N.; Suau, J. M.; Egraz, J. B.; Llauro, M. F.; Ladaviere, C.; Claverie, J. Synthesis and characterization of poly(acrylic acid) produced by RAFT polymerization. Application as a very efficient dispersant of CaCO3, kaolin, and TiO_2. *Macromolecules* **2003**, *36*, 3066.
(8) Moad, G.; Chen, M.; Haussler, M.; Postma, A.; Rizzardo, E.; Thang, S. H. Functional polymers for optoelectronic applications by RAFT polymerization. *Polym. Chem.* **2011**, *2*, 492.
(9) Boyer, C.; Bulmus, V.; Davis, T. P.; Ladmiral, V.; Liu, J. Q.; Perrier, S. Bioapplications of RAFT Polymerization. *Chem. Rev.* **2009**, *109*, 5402.
(10) Boyer, C.; Stenzel, M. H.; Davis, T. P. Building Nanostructures Using RAFT Polymerization. *J. Polym. Sci., Part A: Polym. Chem.* **2011**, *49*, 551.
(11) Perrier, S.; Takolpuckdee, P. Macromolecular design via reversible addition-fragmentation chain transfer (RAFT)/Xanthates (MADIX) polymerization. *J. Polym. Sci., Part A: Polym. Chem.* **2005**, *43*, 5347.
(12) Tan, J.; Sun, H.; Yu, M.; Sumerlin, B. S.; Zhang, L. Photo-PISA: Shedding Light on Polymerization-Induced Self-Assembly. *ACS Macro Lett.* **2015**, *4*, 1249.
(13) Li, M.; De, P.; Gondi, S. R.; Sumerlin, B. S. End group transformations of RAFT-generated polymers with bismaleimides: Functional telechelics and modular block copolymers. *J. Polym. Sci., Part A: Polym. Chem.* **2008**, *46*, 5093.
(14) Beija, M.; Marty, J. D.; Destarac, M. RAFT/MADIX polymers for the preparation of polymer/inorganic nanohybrids. *Prog. Polym. Sci.* **2011**, *36*, 845.
(15) Gody, G.; Zetterlund, P. B.; Perrier, S.; Harrisson, S. The limits of precision monomer placement in chain growth polymerization. *Nat. Commun.* **2016**, *7*, 10514.
(16) Gody, G.; Roberts, D. A.; Maschmeyer, T.; Perrier, S. A New Methodology for Assessing Macromolecular Click Reactions and Its Application to Amine−Tertiary Isocyanate Coupling for Polymer Ligation. *J. Am. Chem. Soc.* **2016**, *138*, 4061.
(17) Kolomanska, J.; Johnston, P.; Gregori, A.; Dominguez, I. F.; Egelhaaf, H. J.; Perrier, S.; Rivaton, A.; Dagron-Lartigau, C.; Topham, P. D. Design, synthesis and thermal behaviour of a series of well-defined clickable and triggerable sulfonate polymers. *RSC Adv.* **2015**, *5*, 66554.
(18) Moskowitz, J. D.; Abel, B. A.; McCormick, C. L.; Wiggins, J. S. High Molecular Weight and Low Dispersity Polyacrylonitrile by Low Temperature RAFT Polymerization. *J. Polym. Sci., Part A: Polym. Chem.* **2016**, *54*, 553.
(19) Ferguson, C. J.; Hughes, R. J.; Nguyen, D.; Pham, B. T. T.; Gilbert, R. G.; Serelis, A. K.; Such, C. H.; Hawkett, B. S. Ab Initio Emulsion Polymerization by RAFT-Controlled Self-Assembly. *Macromolecules* **2005**, *38*, 2191.
(20) Zhang, X.; Boisson, F.; Colombani, O.; Chassenieux, C.; Charleux, B. Synthesis of Amphiphilic Poly(acrylic acid)-b-poly(n-butyl acrylate-co-acrylic acid) Block Copolymers with Various Microstructures via RAFT Polymerization in Water/Ethanol Heterogeneous Media. *Macromolecules* **2014**, *47*, 51.
(21) Jia, Z.; Bobrin, V. A.; Truong, N. P.; Gillard, M.; Monteiro, M. J. Multifunctional Nanoworms and Nanorods through a One-Step Aqueous Dispersion Polymerization. *J. Am. Chem. Soc.* **2014**, *136*, 5824.
(22) Hatton, F. L.; Ruda, M.; Lansalot, M.; D'Agosto, F.; Malmstrom, E.; Carlmark, A. Xyloglucan-Functional Latex Particles via RAFT-Mediated Emulsion Polymerization for the Biomimetic Modification of Cellulose. *Biomacromolecules* **2016**, *17*, 1414.
(23) De la Haye, J. L.; Zhang, X. W.; Chaduc, I.; Brunel, F.; Lansalot, M.; D'Agosto, F. The Effect of Hydrophile Topology in RAFT-Mediated Polymerization-Induced Self-Assembly. *Angew. Chem., Int. Ed.* **2016**, *55*, 3739.
(24) Poon, C. K.; Tang, O.; Chen, X.-M.; Pham, B. T. T.; Gody, G.; Pollock, C. A.; Hawkett, B. S.; Perrier, S. Preparation of Inert Polystyrene Latex Particles as MicroRNA Delivery Vectors by Surfactant-Free RAFT Emulsion Polymerization. *Biomacromolecules* **2016**, *17*, 965.
(25) Huynh, V. T.; Nguyen, D.; Such, C. H.; Hawkett, B. S. Polymer coating of graphene oxide via reversible addition−fragmentation chain transfer mediated emulsion polymerization. *J. Polym. Sci., Part A: Polym. Chem.* **2015**, *53*, 1413.
(26) Pham, B. T. T.; Such, C. H.; Hawkett, B. S. Synthesis of polymeric janus nanoparticles and their application in surfactant-free emulsion polymerizations. *Polym. Chem.* **2015**, *6*, 426.
(27) Charleux, B.; Delaittre, G.; Rieger, J.; D'Agosto, F. Polymerization-Induced Self-Assembly: From Soluble Macromolecules to Block Copolymer Nano-Objects in One Step. *Macromolecules* **2012**, *45*, 6753.
(28) Warren, N. J.; Armes, S. P. Polymerization-Induced Self-Assembly of Block Copolymer Nano-objects via RAFT Aqueous Dispersion Polymerization. *J. Am. Chem. Soc.* **2014**, *136*, 10174.
(29) Canning, S. L.; Smith, G. N.; Armes, S. P. A Critical Appraisal of RAFT-Mediated Polymerization-Induced Self-Assembly. *Macromolecules* **2016**, *49*, 1985.
(30) Mable, C. J.; Warren, N. J.; Thompson, K. L.; Mykhaylyk, O. O.; Armes, S. P. Framboidal ABC triblock copolymer vesicles: a new class of efficient Pickering emulsifier. *Chem. Sci.* **2015**, *6*, 6179.
(31) Canton, I.; Warren, N. J.; Chahal, A.; Amps, K.; Wood, A.; Weightman, R.; Wang, E.; Moore, H.; Armes, S. P. Mucin-Inspired Thermoresponsive Synthetic Hydrogels Induce Stasis in Human Pluripotent Stem Cells and Human Embryos. *ACS Cent. Sci.* **2016**, *2*, 65.
(32) Simon, K. A.; Warren, N. J.; Mosadegh, B.; Mohammady, M. R.; Whitesides, G. M.; Armes, S. P. Disulfide-Based Diblock Copolymer Worm Gels: A Wholly-Synthetic Thermoreversible 3D Matrix for Sheet-Based Cultures. *Biomacromolecules* **2015**, *16*, 3952.
(33) Warren, N. J.; Mykhaylyk, O. O.; Mahmood, D.; Ryan, A. J.; Armes, S. P. RAFT Aqueous Dispersion Polymerization Yields Poly(ethylene glycol)-Based Diblock Copolymer Nano-Objects with Predictable Single Phase Morphologies. *J. Am. Chem. Soc.* **2014**, *136*, 1023.
(34) Mable, C. J.; Gibson, R. R.; Prevost, S.; McKenzie, B. E.; Mykhaylyk, O. O.; Armes, S. P. Loading of Silica Nanoparticles in Block Copolymer Vesicles during Polymerization-Induced Self-Assembly: Encapsulation Efficiency and Thermally Triggered Release. *J. Am. Chem. Soc.* **2015**, *137*, 16098.
(35) Thomas, D. B.; Convertine, A. J.; Hester, R. D.; Lowe, A. B.; McCormick, C. L. Hydrolytic Susceptibility of Dithioester Chain Transfer Agents and Implications in Aqueous RAFT Polymerizations. *Macromolecules* **2004**, *37*, 1735.

DOI: 10.1021/acs.macromol.6b01963
Macromolecules 2017, 50, 182−191

(36) Mertoglu, M.; Laschewsky, A.; Skrabania, K.; Wieland, C. New Water Soluble Agents for Reversible Addition−Fragmentation Chain Transfer Polymerization and Their Application in Aqueous Solutions. *Macromolecules* **2005**, *38*, 3601.
(37) Pissuwan, D.; Boyer, C.; Gunasekaran, K.; Davis, T. P.; Bulmus, V. In Vitro Cytotoxicity of RAFT Polymers. *Biomacromolecules* **2010**, *11*, 412.
(38) Moad, G.; Rizzardo, E.; Thang, S. H. End-functional polymers, thiocarbonylthio group removal/transformation and reversible addition-fragmentation-chain transfer (RAFT) polymerization. *Polym. Int.* **2011**, *60*, 9.
(39) Willcock, H.; O'Reilly, R. K. End group removal and modification of RAFT polymers. *Polym. Chem.* **2010**, *1*, 149.
(40) Shen, W.; Qiu, Q.; Wang, Y.; Miao, M.; Li, B.; Zhang, T.; Cao, A.; An, Z. Hydrazine as a Nucleophile and Antioxidant for Fast Aminolysis of RAFT Polymers in Air. *Macromol. Rapid Commun.* **2010**, *31*, 1444.
(41) Matioszek, D.; Dufils, P.-E.; Vinas, J.; Destarac, M. Selective and Quantitative Oxidation of Xanthate End-Groups of RAFT Poly(n-butyl acrylate) Latexes by Ozonolysis. *Macromol. Rapid Commun.* **2015**, *36*, 1354.
(42) Chong, Y. K.; Moad, G.; Rizzardo, E.; Thang, S. H. Thiocarbonylthio End Group Removal from RAFT-Synthesized Polymers by Radical-Induced Reduction. *Macromolecules* **2007**, *40*, 4446.
(43) Michl, T. D.; Locock, K. E. S.; Stevens, N. E.; Hayball, J. D.; Vasilev, K.; Postma, A.; Qu, Y.; Traven, A.; Haeussler, M.; Meagher, L.; Griesser, H. J. RAFT-derived antimicrobial polymethacrylates: elucidating the impact of end-groups on activity and cytotoxicity. *Polym. Chem.* **2014**, *5*, 5813.
(44) Chen, M.; Moad, G.; Rizzardo, E. Thiocarbonylthio End Group Removal from RAFT-Synthesized Polymers by a Radical-Induced Process. *J. Polym. Sci., Part A: Polym. Chem.* **2009**, *47*, 6704.
(45) Legge, T. M.; Slark, A. T.; Perrier, S. Thermal stability of reversible addition−fragmentation chain transfer/macromolecular architecture design by interchange of xanthates chain-transfer agents. *J. Polym. Sci., Part A: Polym. Chem.* **2006**, *44*, 6980.
(46) Postma, A.; Davis, T. P.; Moad, G.; O'Shea, M. S. Thermolysis of RAFT-Synthesized Polymers. A Convenient Method for Trithiocarbonate Group Elimination. *Macromolecules* **2005**, *38*, 5371.
(47) Mattson, K. M.; Pester, C. W.; Gutekunst, W. R.; Hsueh, A. T.; Discekici, E. H.; Luo, Y.; Schmidt, B. V. K. J.; McGrath, A. J.; Clark, P. G.; Hawker, C. J. Metal-Free Removal of Polymer Chain Ends Using Light. *Macromolecules* **2016**, *49*, 8162.
(48) Pfukwa, R.; Pound, G.; Klumperman, B. POLY 407-Facile end group modification of RAFT made polymers, by radical exchange with hydrogen peroxide. *Abstr. Pap. Am. Chem. Soc.* **2008**, *236*, 1.
(49) Save, M.; Weaver, J. V. M; Armes, S. P.; McKenna, P. Atom Transfer Radical Polymerization of Hydroxy-Functional Methacrylates at Ambient Temperature: Comparison of Glycerol Monomethacrylate with 2-Hydroxypropyl Methacrylate. *Macromolecules* **2002**, *35*, 1152.
(50) Jones, E. R.; Semsarilar, M.; Blanazs, A.; Armes, S. P. Efficient Synthesis of Amine-Functional Diblock Copolymer Nanoparticles via RAFT Dispersion Polymerization of Benzyl Methacrylate in Alcoholic Media. *Macromolecules* **2012**, *45*, 5091.
(51) Blanazs, A.; Ryan, A. J.; Armes, S. P. Predictive Phase Diagrams for RAFT Aqueous Dispersion Polymerization: Effect of Block Copolymer Composition, Molecular Weight, and Copolymer Concentration. *Macromolecules* **2012**, *45*, 5099.
(52) Cunningham, V. J.; Alswieleh, A. M.; Thompson, K. L.; Williams, M.; Leggett, G. J.; Armes, S. P.; Musa, O. M. Poly(glycerol monomethacrylate)−Poly(benzyl methacrylate) Diblock Copolymer Nanoparticles via RAFT Emulsion Polymerization: Synthesis, Characterization, and Interfacial Activity. *Macromolecules* **2014**, *47*, 5613.
(53) Blanazs, A.; Verber, R.; Mykhaylyk, O. O.; Ryan, A. J.; Heath, J. Z.; Douglas, C. W. I.; Armes, S. P. Sterilizable Gels from Thermoresponsive Block Copolymer Worms. *J. Am. Chem. Soc.* **2012**, *134*, 9741.
(54) Mitchell, D. E.; Lovett, J. R.; Armes, S. P.; Gibson, M. I. Combining Biomimetic Block Copolymer Worms with an Ice-Inhibiting Polymer for the Solvent-Free Cryopreservation of Red Blood Cells. *Angew. Chem., Int. Ed.* **2016**, *55*, 2801.
(55) Lovett, J. R.; Warren, N. J.; Ratcliffe, L. P. D.; Kocik, M. K.; Armes, S. P. pH-Responsive Non-Ionic Diblock Copolymers: Ionization of Carboxylic Acid End-Groups Induces an Order−Order Morphological Transition. *Angew. Chem., Int. Ed.* **2015**, *54*, 1279.

DOI: 10.1021/acs.macromol.6b01963
Macromolecules 2017, 50, 182−191